Coral Reefs (2020) 39:1829–1839
https://doi.org/10.1007/s00338-020-02008-3

REPORT

Trophodynamics of the sclerosponge *Ceratoporella nicholsoni* along a shallow to mesophotic depth gradient

Keir J. Macartney[1] · M. Sabrina Pankey[1] · Marc Slattery[2] · Michael P. Lesser[1]

Received: 28 February 2020 / Accepted: 29 September 2020 / Published online: 11 October 2020

Abstract The sclerosponge *Ceratoporella nicholsoni* is a hyper-calcifying high microbial abundance sponge. This sponge has been observed at high densities throughout the Caribbean in the mesophotic zone (30–150 m), as well as cryptic environments in shallow (< 30 m) depths. Given the densities of this sponge, it could play an important role in the cycling of inorganic and organic sources of carbon and nitrogen at mesophotic depths. Additionally, there is broad interest in this sponge as a tool for paleobiology, paleoclimatology and paleoceanography. As a result, it is increasingly important to understand the ecology of these unique sponges in the underexplored Caribbean mesophotic zone. Here we show that this sponge increases in abundance from shallow depths into the mesophotic zone of Grand Cayman Island. We observed no significant differences in the stable isotope signatures of δ^{15}N and δ^{13}C of sponge tissue between depths. A predictive model of sponge diet with increasing depth shows that these sponges consume dissolved organic matter of algal and coral origin, as well as the consumption of particulate organic matter consistent with the interpretation of the stable isotope data. The taxonomic composition of the sclerosponge microbiome was invariant across the shallow to mesophotic depth range but did contain the Phylum *Chloroflexi*, known to degrade a variety of dissolved organic carbon sources. These data suggest that the depth distribution of this sponge may not be driven by changes in trophic strategy and is potentially regulated by other biotic or abiotic factors.

Keywords Mesophotic · Sclerosponge · Microbiome · Stable isotopes · Trophic ecology · Sponge

Topic Editor Alastair Harborne

Electronic supplementary material The online version of this article (https://doi.org/10.1007/s00338-020-02008-3) contains supplementary material, which is available to authorized users.

✉ Keir J. Macartney
kjm1049@wildcats.unh.edu

[1] Department of Molecular, Cellular and Biomedical Sciences and School of Marine Science and Ocean Engineering, University of New Hampshire, Durham, NH 03824, USA

[2] Department of BioMolecular Science, University of Mississippi, Oxford, MS 38677, USA

Introduction

It is well-known that cryptic spaces in coral reefs are a crucial component of overall coral reef productivity (de Goeij and van Duyl 2007; de Goeij et al. 2013, 2017). These habitats may comprise up to 75–90% of total reef volume in the Caribbean (Ginsburg 1983; de Goeij et al. 2017) and are known to be net sinks of dissolved organic matter (DOM), and in particular dissolved organic carbon (DOC). Cryptic spaces also play a significant role in overall productivity of coral reefs and may improve adjacent coral reef health (Slattery et al. 2013). The primary components of cryptobenthic fauna in these habitats are sponges, primarily encrusting species, and the study of cryptic sponges has increased significantly in the last decade due to their potential role as major ecosystem engineers through the sponge loop (de Goeij et al. 2013; 2017). The "Sponge Loop Hypothesis" proposes that sponges consume DOM and produce large concentrations of cellular detritus, such as choanocyte cells, that are subsequently consumed by reef organisms.

The majority of these studies, however, have focused on shallow coral reefs (< 30 m), with far fewer studies on

mesophotic coral reef ecosystems (MCEs; 30–150 m) where endemic communities of sponges can be found in the lower mesophotic (> 60 m) zone of the Caribbean (Lesser et al. 2009; Slattery et al. 2011; Loya et al. 2016). Once exception is a recent study by Lesser et al. (2020) which showed that the encrusting sponge *Halisarca caerulea* produces significantly less detritus at mesophotic depths (~ 50 m) compared to conspecifics at shallow depths (~ 10 m). Since the production of detritus is a prerequisite for a functional sponge loop it demonstrated the broader need to understand the trophic ecology of the sponge fauna found in the low-light environment of MCEs, which may mimic shallow water cryptic spaces, for our overall understanding of the functional ecology of sponges in MCEs.

One of the most understudied members of the sponge community are sclerosponges. Sclerosponges are slow-growing and deposit a calcium carbonate exoskeleton in sequential layers over time, and recent studies have suggested that the symbiotic prokaryotic microbiome of sclerosponges may have an important role in calcification (Garate et al. 2017; Germer et al. 2017). Sclerosponges are found throughout the tropics across a 1000 m depth range and can live for centuries (Lang and Hartman 1975; Benavides and Druffel 1986; Böhm et al. 1996; Swart et al. 1998). One species of sclerosponge, *Ceratoporella nicholsoni* (Fig. 1b), is commonly found within the reef framework, overhangs and small caves of Caribbean MCEs (Lang and Hartman 1975; Santavy et al. 1990; Vacelet et al. 2015). *Ceratoporella nicholsoni* produces a thin layer of siliceous spicule supported tissue over a dense aragonite skeleton (Lang and Hartman 1975; Vacelet et al. 2015). This species of sponge is commonly used for paleoceanographic reconstructions as it produces its skeleton at isotopic equilibrium with surrounding seawater (Benavides and Druffel 1986; Swart et al. 1998, 2002, 2010; Haase-Schramm et al. 2003), but relatively little is known about its general ecology, and trophic ecology in particular. While *C. nicholsoni* can be found at depths shallower than 30 m deep in the reef framework, it is much more common in MCEs below 30 m, where it grows openly on wall faces and overhangs (Lang and Hartman 1975; Vacelet et al. 2015). This particular species is the most conspicuous of the Caribbean sclerosponges (Lang and Hartman 1975; Vacelet et al. 2015) and forms dense communities in the low-light spaces of MCEs, in some cases comprising 25–50% of total cover in overhangs and small caves (Lang and Hartman 1975). At depths below 70 m, this sponge and

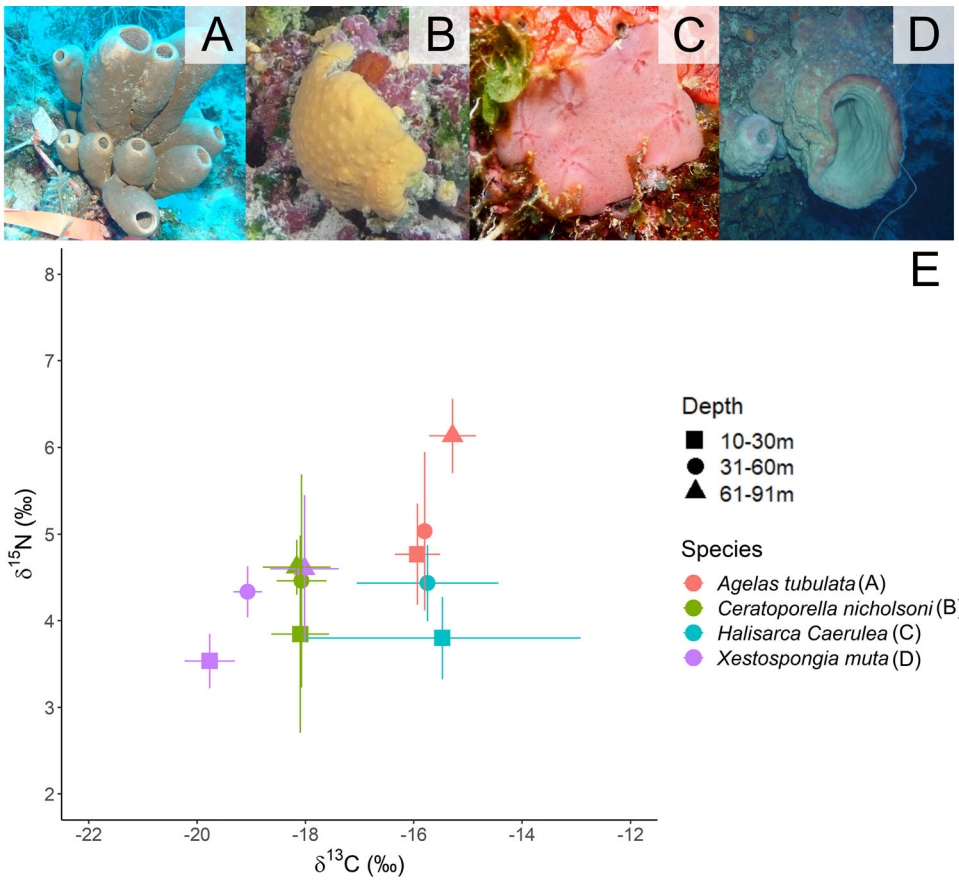

Fig. 1 In-situ photos of A) *Agelas tubulata* (photo: Liz Kintzing), B) *Ceratoporella nicholsoni* (photo: Keir Macartney), C) *Halisarca caerulea* (photo: Sabrina Pankey) and D) *Xestospongia muta* (photo: Michael Lesser. E) Comparative bivariate plot of Caribbean coral reef sponge bulk $\delta^{13}C$ and $\delta^{15}N$ values (mean ± SD) along a shallow to mesophotic depth gradient from published literature. All data was binned to match the binning of depths in this publication. Data for *X. muta* were taken from Morrow et al. (2016), data for *A. tubulata* was taken from Slattery et al. (2011) and data for *H. caerulea* was taken from Lesser et al. (2020)

potentially other less common sclerosponge species may contribute significantly to the emergent deep reef community and its structure (Lang and Hartman 1975; Swart et al. 1998; Vacelet et al. 2015) by assuming the functional role of scleractinian corals as reef. Since this sponge is classified as a high microbial abundance (HMA) sponge (Santavy et al. 1990), it is very likely utilizing DOM in its diet (Yahel et al. 2003; de Goeij et al. 2013, 2017; Mueller et al. 2014). As a result, these sponges may contribute to DOM cycling (i.e., Sponge Loop) on MCEs.

As an HMA sponge the prokaryotic microbiome of *Ceratoporella nicholsoni* likely plays a significant role in its trophic ecology as reported for many HMA sponges (Hentschel et al. 2012; Pita et al. 2018), and specifically its ability to assimilate and translocate particulate organic matter (POM) and DOM for growth. Recent research has shown that detritus production is linked to the quantity of the POM and DOM available, and consumption of these resources relies on both the host and its microbiome (de Goeij et al. 2013, 2017; Mueller et al. 2014; Rix et al. 2016; Lesser et al. 2020). Additionally, the microbiome in many sponges is responsible for the production of secondary metabolites (Taylor et al. 2007; Hentschel et al. 2012; Pita et al. 2018), and given the slow growth of *C. nicholsoni*, these compounds could be important in the prevention of overgrowth by competitors. While previous studies have analyzed the C. *nicholsoni* microbiome using traditional media-based isolation techniques (Santavy et al. 1990), many sponge-associated microbes are nonculturable. The use of metagenetic techniques can increase both the recovery and resolution of the *C. nicholsoni* microbiome, and its potential function. Here we utilize bulk stable isotope techniques (SIA) and a diet reconstruction model, as well as 16s rRNA amplicon sequencing and predicted metagenomic content in order to characterize the community composition, potential function and the trophic ecology of these unique sponges at both shallow and mesophotic depths in the Cayman Islands. We hypothesize that this sponge will increase in abundance in the Grand Cayman mesophotic zone, that its diet will be a reflection of the available food resources and that its microbiome will have broad metabolic potential, as observed in other sponges.

Methods

Site description

Samples of the sclerosponge *C. nicholsoni* were collected on reefs in the vicinity of the Kittiwake Anchor Buoy site, Grand Cayman (Lat: 19.362756, Long: − 81.402437) along a shallow to mesophotic (10–100 m) depth gradient on Grand Cayman Island (Fig. S1). This site exhibits a spur and grove structure with a sloping reef structure between 15–60 m, at which point reef topography turns into a vertical wall. Additionally, based on data collected previously at this site (Lesser et al. 2019) the concentrations (μmol l^{-1}) of POC and PON increase significantly as depth increases into the mesophotic zone, while DOC and DON decrease significantly as depth increases (Lesser et al. 2019).

Sample collection

Samples were collected in January 2019 by divers utilizing mixed gas closed circuit rebreather systems and technical diving procedures for collection deeper than 30 m while open-circuit SCUBA was used to collect samples above 30 m. Whole sponges were removed from the substrate using a hammer and chisel, brought to the surface in plastic bags, transported in seawater to a wet laboratory and immediately frozen at − 4 °C. Samples were transported to the University of New Hampshire while frozen for further analysis and stored at − 80 °C Samples were binned into groups from 10–30 m (shallow) (n = 8), 31–60 m (upper mesophotic) (n = 5) and 61–90 m (lower mesophotic) (n = 9) where the seawater temperatures at approximately the mid-point of each depth grouping was 27.12 °C at 22 m, 27.32 °C at 46 m and 27.49 °C at 76 m with temperatures measured as described in Lesser et al. (2009). Photosynthetically active radiation (PAR: μmol quanta m^{-2} s^{-1}) decreases significantly at this site as depth increases into the mesophotic with irradiances at approximately the midpoint of each depth bin of 22 m = 263 μmol quanta m^{-2} s^{-1}, 46 m = 126 μmol quanta m^{-2} s^{-1}, and 76 m = 61 μmol quanta m^{-2} s^{-1} with irradiances measured as described in Lesser (2018).

Sclerosponge surveys

Sclerosponge abundance and percent cover were measured using replicate transects (n = 3) of 30 m length at depths of 37, 49, 67, 81 and 97 m, with1 m^2 quadrats (n = 5) positioned at random points along each transect. Since sclerosponges are primarily found in more cryptic environments (e.g., overhangs), these depths were chosen based on the presence of relevant habitat. It was not possible to enumerate sclerosponges with any degree of accuracy in the cryptic habitat at < 30 m. Specifically, each transect line began at an identified overhang where a 1 m^2 quadrat was placed. Following that, a random number generator was used to determine the next overhang to be analyzed (i.e., using numbers from one to five if the random number was "3" then the third overhang from the transect origin was measured). For each transect, at all

depths, the number of overhangs analyzed was $n = 5$. All sclerosponges within each m^2 quadrat were counted, and the percent cover of these sclerosponges was estimated using the point intercept method.

Stable isotope analysis

Samples of *C. nicholsoni* tissue were taken by using a sterile razor to scrape tissue from the surface of the sponge. Tissue samples were dried at 55 °C for 24 h before pulverizing into a powder using a mortar and pestle. Samples of tissue were sent to the Marine Biological Laboratory (Woods Hole, MA) for the bulk analysis of particulate C and N as well as the natural abundance of the stable isotopes δ^{15}N and δ^{13}C. Prior to analysis samples were acidified using 1N HCL. Samples were analyzed using a Europa ANCA-SL elemental analyzer-gas chromatograph attached to a continuous-flow Europa 20–20 gas source stable isotope ratio mass spectrometer. The carbon isotope results are reported relative to Vienna Pee Dee Belemnite and nitrogen isotope results are reported relative to atmospheric air and both are expressed using the delta (δ) notation in units per mil (‰). The analytical precision of the instrument is ± 0.1‰, and the mean precision of sample replicates for δ^{13}C was ± 0.4 ‰ and δ^{15}N was ± 0.2 ‰. In order to avoid changes in δ^{15}N due to acidification (Schubert and Nielsen 2000), non-acidified tissue samples were sent to the Stable Isotope Laboratory at the University of Miami's Rosenstiel School of Marine Geosciences. The δ^{15}N of non-acidified samples was determined using a Costech CN analyzer interfaced to a Thermo Advantage V with δ^{15}N standards supplied from the International Atomic Energy Authority (IAEA) (sensu Mackenzie et al. 2015). Statistical analyses for differences between depths for all SIA variables were conducted utilizing ANOVA in R statistical software (version 3.4.2). Any variables not meeting the assumptions of normality were log transformed before analysis. The relative diet contribution was assessed using the R package "SIAR4" (Parnell et al. 2010) sensu Lesser et al. (2020). Source endmember values for algal DOM (δ^{13}C: − 15.42‰, δ^{15}N: 0.80‰), coral DOM (δ^{13}C: − 18.19‰, δ^{15}N: 0.26‰), and coral reef POM (δ^{13}C: − 24.91‰, δ^{15}N: 5.62‰) were taken from (van Duyl et al. 2011a, 2018) and values for sponge derived detritus (δ^{13}C: − 19.54‰, δ^{15}N: 2.56‰) were taken from (Lesser et al. 2020). For the effects of depth in the mixing model both δ^{13}C and δ^{15}N stable isotope values for *Lobophora variegata* (Slattery and Lesser 2014) and *Montastraea cavernosa, Montastraea annularis* (now *Orbicella annularis*) and *Agaricia agaricities* (Lesser et al. 2010; Muscatine et al. 1989; Muscatine and Kaplan 1994) were included as averaged source endmembers for algal and coral DOM for their respective depths. The source endmember data were taken from different sites in the Caribbean and are consistent with the known variation of these endmember isotope values throughout the region and between depths (e.g., Lesser et al. 2020). The trophic enrichment factor applied for δ^{13}C was 0.5 ± 0.5%, and for δ^{15}N a trophic enrichment factor of 3.0 ± 0.5% was applied sensu van Duyl et al. (2018) and Lesser et al. (2020).

DNA Isolation and 16 s rRNA amplicon sequencing

To obtain microbial genomic DNA, *C. nicholsoni* tissue was removed from the calcareous skeleton using a sterile razor with care taken to avoid inclusion of $CaCo_3$ debris from the skeleton into the sample. Approximately 200–300 mg of tissue were removed. Sponge DNA was isolated using a Qiagen DNeasy PowerSoil extraction kit with the manufacture's protocol modified as follows. Sponge tissue was added to the PowerSoil bead tubes with 5 µl of Proteinase K (20 mg/ml stock in 10% SDS) and 2 µl of RNAse (Qiagen) before incubation at 55 °C for 18 h. After incubation, PowerSoil Kit Solution 1 was added, and samples subsequently underwent a bead beating step using a Qiagen Tissue Lyser for 5 min at 50 Hz. The Qiagen DNeasy PowerSoil kit standard instructions were followed post-bead beating to produce DNA samples.

Microbial DNA was amplified using the polymerase chain reaction (PCR) with primer sets targeting the universal prokaryotic 16S rRNA gene. Degenerate primers designed to amplify the hypervariable region V3–V4 of the 16S rRNA gene were used and included a forward primer 515F (5′-GTGYCAGCMGCCGCGGTAA; Parada et al. (2016)) and reverse primer 806R [5′-GGACTACNVGGGTWTCTAAT; Apprill et al. (2015)]. Fluidigm linker sequences CS2 (5′-ACACTGACGACATGGTTCTACA) and CS2 (5′-TACGGTAGCAGAGACTTGGTCT) were added to the 5′ end of both forward and reverse primers to facilitate Illumina MiSeq. The 16S rRNA gene PCR consisted of a 25 µl reaction with 12.5 µl AmpliTaq Gold 360 Master Mix (Applied Biosystems), 1.0 µl GC-enhancer, 0.5 µl 515F (10 µM) and 0.5 µl 806R (10 µM), 2.0 µl of DNA template (40–60 ng) and 8.5 µl nuclease free water (Integrated DNA Technologies, Coralville, Iowa). Reactions were performed using the following protocol: initial denaturation for 10 min at 95 °C, 30 cycles of 95 °C for 45 s, 50 °C for 60 s, and 72 °C for 90 s, followed by a 10 min extension at 72 °C. The PCR products were then electrophoresed on a 1% agarose gel. The 16S rRNA PCR amplicons containing Fluidigm linkers were sequenced on an Illumina MiniSeq System employing V2 chemistry (2 × 150 bp reads) at the University of Illinois at Chicago (UIC) Research Resources Center's Sequencing Core. The amplicon sequence variants (ASVs)

were inferred and tabulated across sclerosponge samples using "DADA2" (Callahan et al. 2016) using an established bioinformatic pipeline (Lesser et al. 2020).

Analyses of the microbial communities of *C. nicholosoni* were done utilizing the R package "PhyloSeq" (McMurdie and Holmes et al. 2015) in R sensu (Lesser et al. 2020). Samples with fewer than 10,000 counts were filtered from the ASV count table. Additionally, ASVs detected in more than two samples and had at least 10 occurrences across samples were retained during the filtering process. The samples were then rarefied in order to account for sampling effort. To test alpha diversities, the Shannon richness index was used. Ordination plots were produced based on Bray–Curtis distances using nonmetric multidimensional scaling (NMDS) (Stress value = < 0.0001). To assess compositional differences at varying taxonomic scales, the rarefied ASV count table was consolidated by rank using the PhyloSeq "tax_glom" function and then raw counts were transformed to center log rations using the "transform" function (CLR) from the R package "microbiome" (Callahan et al. 2016). Compositional differences between depths were tested using PERMANOVA with the Adonis function from the R package "vegan". Any differences observed during post hoc testing at phylum level for taxa between depths were tested using ANOVA and Tukeys HSD. Raw 16S rRNA reads were submitted to the NCBI Sequence Read Archive under BioProject accession number PRJNA555077.

Metagenomic functional abundances were predicted using "PICRUSt2" v2.1.0–b (https://github.com/picrust/picrust2/wiki) (Langille et al. 2013; Langille 2018). The 16S rRNA ASVs inferred by DADA2 were aligned with "HMMER" (Eddy 2008) and then placed in a reference tree provided by PICRUSt2 using "EPA–ng" and "GAPPA" (Barbera et al. 2019). Gene family numbers were predicted for 16S rRNA as well as KEGG functions (i.e., EC and KO accessions) using Hidden State Prediction ("castor") based on 16S rRNA ASV abundances and phylogenetic proximity to reference taxa with available genomes. In order to minimize error in gene content prediction due to poor matches to available genomes, any ASVs receiving Nearest-Sequenced-Taxon-Index (NSTI) scores below two were removed from subsequent analyses. Abundances of biological pathways encoded by microbiomes were then predicted using MinPath (Ye and Doak 2009). Abundances of KEGG genes of interest and all pathways from "MetaCyc" inferences were assessed for differences between depth zones using ANOVA on relative abundances normalized to the total reads in the sample. KEGG genes of interest were selected to assess carbon and nitrogen metabolism, secondary metabolite production and indications of stress, such as genes encoding for heat shock proteins.

Results

Sclerosponge surveys

Both percent cover (ANOVA: $F_{4,14} = 82.33$, $P < 0.0001$) and abundance per m^{-2} (ANOVA: $F_{4,14} = 100.01$, $P < 0.0001$) of *C. nicholsoni* significantly increased with depth from the upper mesophotic zone (31–60 m) to the lower mesophotic zone (61–90 m) (Fig. 2). At lower mesophotic depths sponges were both more abundant and had significantly greater percent cover than those found in the upper mesophotic zone (Tukey's HSD, $P < 0.05$), and were qualitatively larger than their shallow-water counterparts inferred based on fewer individuals per m m^{-2} but increased percent cover.

Stable isotopes

There were no significant differences between the sclerosponge tissue $\delta^{13}C$ (ANOVA: $F_{2,19} = 0.061$, $P = 0.941$), $\delta^{15}N$ (ANOVA: $F_{2,19} = 1.4907$, $P = 0.25$) or C:N ratios (ANOVA: $F_{2,19} = 0.912$, $P = 0.418$) as a function of depth (Fig. 1e, Table S1). A non-significant enrichment between ~ 0.5–1.0‰ was found for acidified samples (Table S2), similar to previous results (Kolasinski et al. 2008). We used the results from non-acidified samples for all downstream analyses. The SIAR4 diet reconstruction shows high variability in source contributions to sclerosponge diets and there were no significant differences between depths in the reconstructed diets (Fig. 3,

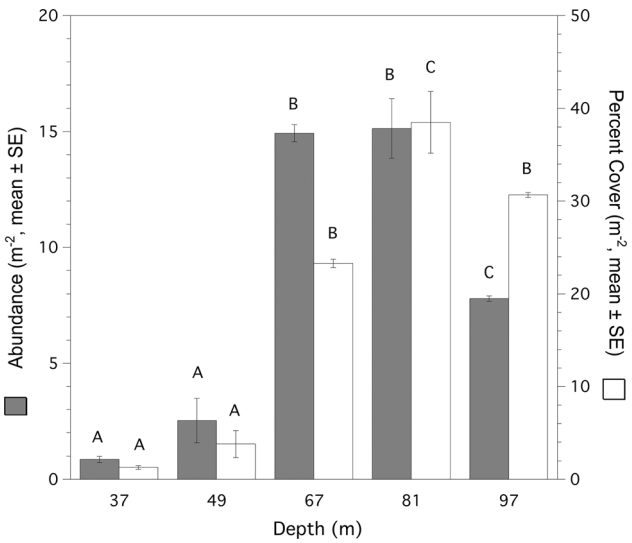

Fig. 2 Depth dependent mean abundance (± SE) and percent cover (± SE) per m^2 of benthic substrate for *Ceratoporella nicholsoni* in the Grand Cayman mesophotic zone. Post hoc multiple comparison testing reveals depths with common superscripts are not significantly different from each other (Tukey's HSD, $P < 0.05$) for both mean abundance and mean percent cover

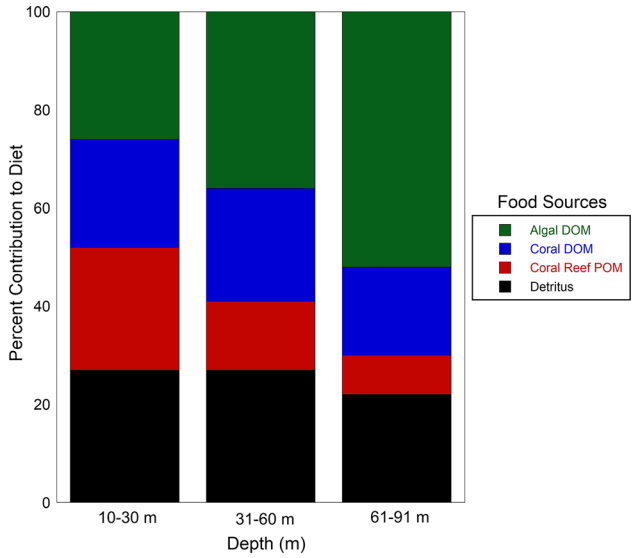

Fig. 3 Bayesian diet reconstruction of *Ceratoporella nicholsoni* diet along a shallow to mesophotic depth gradient showing the mean percent contribution of each food source to the *C. nicholsoni* diet

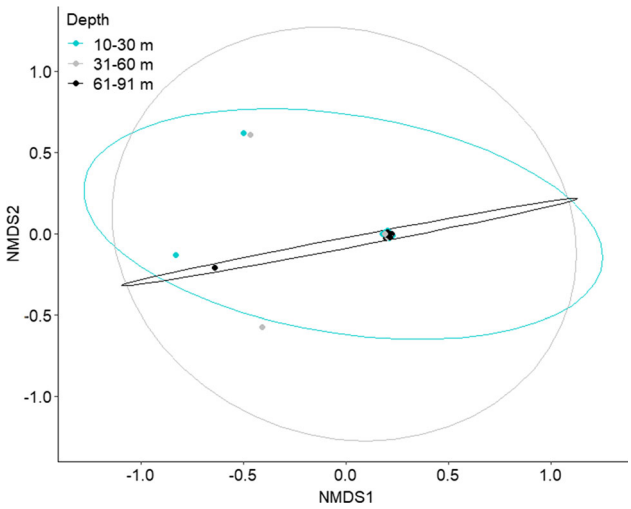

Fig. 4 Multidimensional analysis of the β-diversity estimates using Bray–Curtis distance matrices of ASV composition for *Ceratoperlla nicholsoni* microbial community composition between depths. The 95% confidence interval (CI) ellipses are drawn to show the depth groupings

Table S3). There is, however, a larger contribution of benthic derived DOM in *C. nicholosoni*, with coral and algal DOM contributing approximately 40–70% to the total diet compared to POM. And there is an increase in both algal and coral DOM in the diet of these sponges as depth increases into the mesophotic zone (Fig. 3, Table S3), while live and detrital POM contributes approximately 20–50% to the diet which decreases with increasing depth (Fig. 3, Table S3).

16s rRNA metabarcoding and predictive functional profiling

A total of 805,756 16S rRNA MiniSeq read-pairs were initially recovered from sequencing. After merging and quality trimming with DADA2, 692, 894 read-pairs remained.

These ranged from 37,833 to 19,217 with a mean of 30,125 ± 3,720 reads per sample. A total of 858 unique ASVs were initially recovered, but ASVs unique to a single sample or with fewer than 5 total observations were removed from the dataset, resulting in a total of 412 unique ASVs for downstream analyses.

The multidimensional analysis of the Beta diversity using Bray–Curtis distance matrixes showed no significant difference between microbial community ASV composition between depth zones (PERMANOVA: $F_{2,19} = 0.893$, $P = 0.54$) (Fig. 4). Both phyletic composition (PERMANOVA: $F_{2,19} = 1.597$, $P = 0.063$) and class level composition (PERMANOVA: $F_{2,19} = 0.901$, $P = 0.578$) did not differ significantly between depths With the exception of the Phylum *Dadabacteria*, no significant differences in overall phyletic abundance between depth zones were found in *C. nicholsoni* (Fig. S2). There were significant differences between depths in the *Dadabacteria* (PERMANOVA: $F_{2,19} = 5.13$, $P = 0.015$) (Fig. S2), for which higher total counts were observed in mesophotic compared to shallow depths (Tukeys HSD < 0.05). In the microbiomes of sampled *C. nicholsoni* 84% of the reads belong to ASVs of the following 5 phyla; *Chloroflexi* (32%, ± 5%, mean ± SD), *Thaumarcheaota* (16% ± 5%), *Proteobacteria* (15%, ± 3%), *Acidobacteria* (12%, ± 4%) and *Actinobacteria* (9%, ± 2%) (Fig. S3). Within the *Chloroflexi* phylum, classes "TK17" and *Dehalococcoidia* made up 12% ± 3% and 10% ± 4% of the total microbiome respectively (Fig. 5, S4). Within the *Thaumarcheota*, the *Nitrososphaeria* comprise 15% ± 4% of the total microbiome (Fig. 5, S4). The Proteobacteria are dominated by the *Gammaproteobacteria* and the *Alphaproteobacteria*, comprising 7% ± 2% and 4% ± 1%, respectively, of the total microbiome. Within the *Acidobacteria*, dominant classes include the *Acidobacteriia* (3% ± 2% of total microbiome) and "Subgroup 9" (4% ± 2% of total microbiome). The *Actinobacteria* are almost exclusively composed of the class *Acidimicrobiia*, which is 8% ± 3% of the total microbiome of *C. nicholsoni* (Fig. 5, S4). The Shannon-Alpha diversity of all sponges ranged between 4.78 and 3.42 but there were no significant differences between depths (ANOVA: $F_{2,19} = 0.282$, $P = 0.758$) (Fig. S5).

Functional profiling between depths was accomplished with PICRUSt2. The mean NSTI score was 0.41 ± 0.061 (mean ± SD) and ranged between 0.31 and 0.54. There were significant differences in mean NSTI scores between

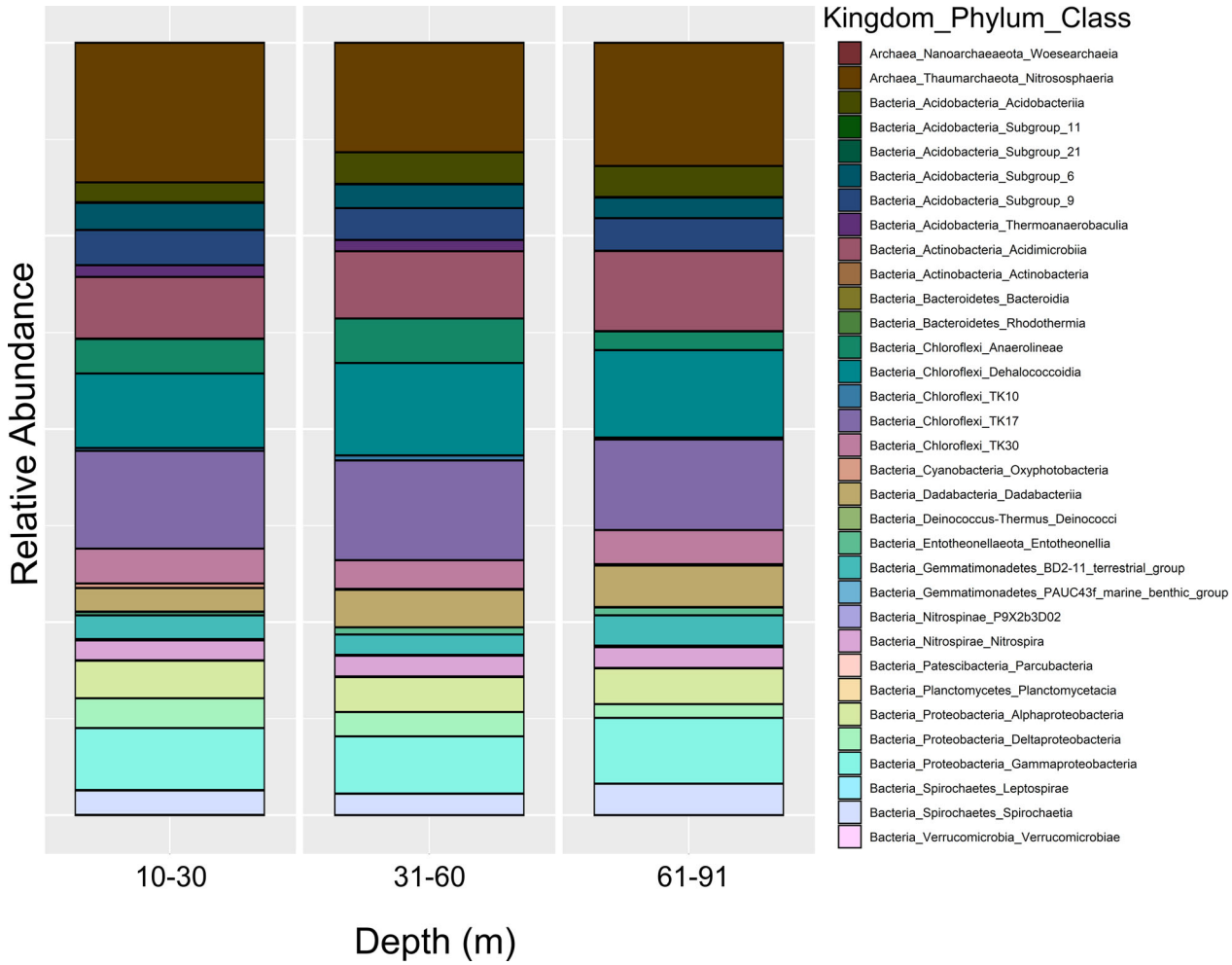

Fig. 5 Average relative abundance (percentage) at the Class level for the community composition of the *Ceratoporella nicholsoni* microbiome along a shallow to mesophotic depth gradient

depths (ANOVA: $F_{2,19} = 5.931$, $P = 0.009$), with shallow samples returning higher scores (0.47) compared to the lower and upper mesophotic samples (Tukey's HSD = < 0.05). The analysis returned 238 MetaCyc pathways and 4051 unique KO genes. Of the 238 pathways, only pathway "GLYCOGENSYNTH-PWY" (glycogen biosynthesis I (from ADP-D-Glucose)) had significant enrichment in the pathway for shallow depths compared to lower mesophotic depths (ANOVA: $F_{2,19} = 0.971$, FDR adjusted $P = 0.022$). KEGG genes of interest (Table S1) were tested for differences between depths and while no significant differences were found (ANOVA: FDR adjusted $P > 0.05$), all genes of interest (Table S4) were present in the inferred metagenome of the samples.

Discussion

The percent cover surveys of *C. nicholsoni* in Grand Cayman follow a similar pattern to the percent cover observed for *C. nicholsoni* in Discovery Bay, Jamaica described by Lang and Hartman (1975). Our study shows *C. nicholsoni* occupies approximately 25 to 35% of relevant habitat space (i.e., wall overhangs and small caverns) between the depths of 67 to 97 m, making it one of the dominant members of the community on Grand Cayman lower mesophotic reefs. This pattern of distribution is similar to those seen in non-calcareous siliceous sponges on open habitat space in the mesophotic throughout the Caribbean (Lesser 2006; Lesser et al. 2009, 2019; Slattery and Lesser 2015; Lesser and Slattery 2018). That distribution is influenced by food availability, both DOM and POM, but nitrogen-rich POM that increases in quantity with depth is believed to be essential for the development and maintenance of increasing sponge biomass with

increasing depth. (Lesser 2006; Trussell et al. 2006; Lesser et al. 2009; Lesser and Slattery 2018; Slattery et al. 2011; Slattery and Lesser 2015; Morrow et al. 2016). As sclerosponges are considered low-light species, found primarily in the reef framework at depths shallower than 50 m (Lang and Hartman 1975; Vacelet et al. 2015), and below large overhangs and caverns in the lower mesophotic (Lang and Hartman 1975) the factors that influence emergent sponge distributions may not regulate sclerosponge distributions. Here we addressed whether the trophic ecology of these sponges is similar to that of open reef sponges where food quality and quantity play an important role in the ecological depth distributions of sponges throughout the Caribbean (Lesser and Slattery 2018; Lesser and Slattery 2018).

The stable isotopes of *C. nicholsoni* do not reveal any significant depth-dependent changes (Fig. 1e) in trophic strategy, which is contrary to previous studies of sponges where stable isotopic signatures in the mesophotic show clear patterns of enrichment with depth, and often transitions from photoautotrophy to heterotrophy (Slattery et al. 2011; Morrow et al. 2016; Lesser et al. 2020). Previous studies have shown significant increases in $\delta^{15}N$ between shallow and mesophotic depths (Fig. 1e) in *Xestospongia muta* (Fig. 1d), *Agelas tubulata* (Fig. 1a) and *Halisarca caerulea* (Fig. 1c) indicating a shift from photoautotrophic resources to heterotrophic resources such as bacterioplankton, which are more abundant in the mesophotic (Lesser 2006; Lesser et al. 2019, 2020). The emergent sponges *X. muta* and *A. tubulata* also showed significant increases in $\delta^{13}C$ (Fig. 1e) which in *X. muta* has been hypothesized to be the result of the decrease of photoautotrophic cyanobacteria in the microbiome as depth increases (Morrow et al. 2016). The encrusting and generally cryptic sponge *H. cearulea* did not have a significant decrease in $\delta^{13}C$ (Fig. 1e) in a study by Lesser et al. (2020), which is similar to the patterns observed for *C. nicholsoni,* and potentially due to the low-light environments they are found in.

The close grouping of the isotopic signatures from *C. nicholsoni* (Fig. 1e, Table S1) indicates that contributions to their diet from their microbiome and the consumption of DOM and POM in these sponges are similar throughout their depth distribution. The values for these sponges $\delta^{13}C$ (~ -18‰) are slightly higher than those typically found in marine phytoplankton (-19 to -24‰) but within the typical range for DOM (-16 to -23‰) (Fry 2006; Slattery et al. 2011; van Duyl et al. 2011, 2018; Lesser et al. 2020). The $\delta^{15}N$ (~ 4.5‰) of the sampled sclerosponges is similar to the range for both bulk POM and DOM (1–6‰) (Fry 2006; Slattery et al. 2011; van Duyl et al. 2011, 2018; Ren et al. 2012). Taken together, it appears this sponge is dependent primarily on DOM as a carbon source, as observed in the diet reconstruction, but does consume picoplankton as do many HMA sponges (de Goeij et al. 2017; McMurray et al. 2018). The $\delta^{13}C$ and $\delta^{15}N$ values for this sponge are similar to open reef HMA sponges from shallow waters (Fig. 1e) (Freeman and Thacker 2011; van Duyl et al. 2011, 2018; Morrow et al. 2016; Lesser et al. 2020). The diet reconstruction for the sclerosponges indicates a reliance on DOM (60–70%) from benthic primary producers with the remainder of the diet made up of live and detrital POM. While there is a large amount of variation in the diet reconstruction model (Table S3), it supports the stable isotope results, and its interpretation. However, this sponge does appear to consume more detrital matter and POM (Fig. 3) compared to a diet reconstruction from *H. caerulea* (Lesser et al. 2020) which is likely a reflection of this sponge's unique microbial community and the nutrient cycling processes found within that community. For instance, we do not know whether the microbiome of *C. nicholsoni* is involved in the uptake of DOM and its re-synthesis and translocation to the host as amino acids as observed in other sponge species (Fiore et al. 2013, 2015; Shih et al. 2020). It should be noted that the diet reconstruction (Fig. 3) is based on endmember values from other taxa or geographic areas, but no direct feeding measurements were made in this study and none are available from the literature for sclerosponges. Feeding studies should be done to validate the diet reconstruction model presented here.

The amplicon sequencing of 16s rRNA provides some insights into the metabolic functions and nutrient cycling in the sponge holobiont. The microbial community and the dominant taxa found in *C. nicholsoni* are similar to other prokaryotic microbiome communities in the Demospongiae (Thomas et al. 2016; Bayer et al. 2018; Pita et al. 2018). Interestingly, the *Chloroflexi* are the most abundant phyla in these sclerosponges, with higher abundances then observed in other HMA sponge microbiomes (Thomas et al. 2016; Pita et al. 2018). Specifically, in the order *Agelasida*, where *C. nicholsoni* is classified, *Chloroflexi* are often found in high abundances in sponges, generally between 10–29% (Bayer et al. 2018). The metagenomes of *Chloroflexi* from sponges show wide metabolic diversity that includes the ability to fix carbon under aerobic an anaerobic conditions, conduct ammonia and nitrite uptake, as well as other precursors for multiple biochemical pathways including amino acid biosynthesis (Bayer et al. 2018) which could subsequently be translocated to the host (sensu Shih et al. 2020). In particular, complex carbohydrate degradation pathways have been reported in *Chloroflexi,* and other members of the prokaryotic microbiome of sponges, which may enhance their ability to utilize the DOM pool on coral reefs (Slaby et al. 2017; Bayer et al. 2018). Bayer et al. (2018) also found that the *Chloroflexi*

have the genomic potential for degradation of DOM, both its recalcitrant and labile forms. Additionally, the presence of *Thaumarcheota* in *C. nicholsoni* is not surprising as it is the most abundant archaeal phyla in HMA sponges (Thomas et al. 2016; Pita et al. 2018). Recent research on the *Thaumarchaeota* has shown that this phylum may be a keystone microbial taxa in some sponges, where it has the ability for ammonia oxidation (e.g., Engelberts et al. 2020).

The functional inference provided by the PICRUSt2 analysis of the prokaryotic microbiome supports the potential of these sponges to use multiple complex carbon, nitrogen and sulfur cycling pathways. Weighted NSTI scores serve as a method of testing the reliability of such predictions (Langille et al. 2013), which calculates dissimilarity between available reference genomes and the predicted metagenome. The NSTI scores in this study were high, with a mean score of 0.41 and shallow scores being the highest, at 0.47, compared to 0.37 for upper mesophotic and 0.38 for lower mesophotic samples. These particular scores are relatively high compared to previous PICRUSt analyses on sponge samples, being twice as high as those analyzed by Cleary et al. (2015). Higher NSTI scores generally result in lower predictive accuracy, but a recent study by Fiore et al. (2020) showed that despite moderate NSTI values (0.15–0.32), a PICRUSt analysis of the sponge *Xestospongia muta*, showed a strong correlation between the functional profiles of its metatranscriptome and the functional predictions for both coverage and abundance. This suggests that functional analyses such as PICRUSt2 may still provide meaningful predictions, even in some poorly characterized communities (i.e., sponge microbiomes).

The only significant difference between depths for both MetaCyc pathways and selected KEGG genes was the glycogen synthesis pathway, which was enriched in shallow samples relative to the lower mesophotic. However, multiple pathways and KEGG genes related to nitrogen, carbon, sulfur and phosphorous cycling were found to be abundant (Table S4), with the exception of photoautotrophic pathways. Genes for polyketide synthase and non-ribosomal peptides synthesis were also found, indicating the sponge microbiome has the capability for chemical defense of this sponge, potentially for prevention of predation or allelopathic interactions with faster growing competitors (Pawlik 2011; Trindade-Silva et al. 2013; Slattery et al. 2016; Gutleben et al. 2019). The *Chloroflexi* also have the potential to participate in sponge chemical defense (Gutleben et al. 2019), and their high abundances may provide this slow-growing sponge secondary metabolites to prevent overgrowth by competitors for space. These chemical compounds may be present at all depths, based on the predictive functional profiling, which would indicate that this sclerosponge does not require an increase in chemical defenses along the depth gradient. Such a finding would imply that predation or competitive allelopathic interactions are similar at all depths, unlike previous observations of varying chemical defenses in sponges from the shallow to mesophotic zone (e.g., Slattery et al. 2016).

Conclusions

Here we have shown that the sclerosponge, *C. nicholsoni*, similar to observations of sponge communities on coral reefs in the Caribbean (Lesser and Slattery 2018), does show an increase in percent cover and abundance into the mesophotic zone but that its microbiome community is invariant along the shallow to mesophotic depth gradient. The abundance of this sponge, and the metabolic diversity of its microbiome, at mesophotic depths suggests that this sponge may play a previously underappreciated role in DOM cycling in these deep, low-light habitats. Additionally, it appears that this sponge does not change its trophic strategy with depth based on the stable isotope analyses and diet reconstruction model, which is contrary to previous studies on sponges, and some scleractinian corals, in the mesophotic. Factors such as its preference for low-light habitats and the energetic requirements (i.e., ion pumping) of calcification may be why this sponge exhibits an unexpected pattern in its trophic ecology compared to siliceous demosponges in the Caribbean. Other factors such as sedimentation (given their preference for overhangs and vertical walls in the mesophotic), competition or mesophotic reef geomorphology (vertical wall versus slopes) could regulate this sponge's distribution as suggested by Lang and Hartman (1975). In particular, direct feeding studies on this sponge will be necessary for validating the diet reconstruction and isotope signatures presented here. Given the continuing interest in this sponge as an indicator species for paleobiology, paleoclimatology and paleoceanography, understanding its ecology and potential roles it plays on coral reefs at all depths will be critical for understanding the dynamics of MCEs.

Acknowledgements We thank K. Morrow, E. Kintzing, and D. Gochfeld for field and laboratory support. We thank A. Weinheimer for insightful comments on the manuscript draft and statistical analyses. We thank Dr. Peter Swart for his comments on the manuscript, and for re-running non-acidified sponge tissue samples at the University of Miami's Rosenstiel School of Marine Geosciences. All sample collections complied with the laws of the Cayman Islands and the United States of America. Support was provided by NSF Biological Oceanography (OCE–1632348/1632333) to MPL and MS respectively, and the University of New Hampshire Marine Biology Small Grants fund to KJM.

Compliance with ethical standards

Conflict of interest On behalf of all authors, the corresponding author states that there is no conflict of interest.

References

Apprill A, McNally S, Parsons R, Weber L (2015) Minor revision to V4 region SSU rRNA 806R gene primer greatly increases detection of SAR11 bacterioplankton. Aquat Microb Ecol 75:129–137

Barbera P, Kozlov AM, Czech L, Morel B, Darriba D, Flouri T, Stamatakis A (2019) EPA-ng: massively parallel evolutionary placement of genetic sequences. Syst Biol 68:365–369

Bayer K, Jahn MT, Slaby BM, Moitinho-Silva L, Hentschel U (2018) Marine sponges as *Chloroflexi* hot spots: genomic insights and high-resolution visualization of an abundant and diverse symbiotic clade. mSystems 3:1–19

Benavides LM, Druffel ERM (1986) Sclerosponge growth rate as determined by 210Pb and Δ14C chronologies. Coral Reefs 4:221–224

Böhm F, Joachimski MM, Lehnert H, Morgenroth G, Kretschmer W, Vacelet J, Dullo WC (1996) Carbon isotope records from extant Caribbean and South Pacific sponges: Evolution of δ13C in surface water DIC. Earth Planet Sci Lett 139:291–303

Callahan BJ, Sankaran K, Fukuyama JA, McMurdie PJ, Holmes SP (2016) Bioconductor workflow for microbiome data analysis: from raw reads to community analyses. F1000Research 5:1492

Cleary DFR, de Voogd NJ, Polónia ARM, Freitas R, Gomes NCM (2015) composition and predictive functional analysis of bacterial communities in seawater, sediment and sponges in the Spermonde Archipelago, Indonesia. Microb Ecol 70:889–903

de Goeij JM, van Duyl FC (2007) Coral cavities are sinks of dissolved organic carbon (DOC). Limnol Oceanogr 52:2608–2617

de Goeij JM, Lesser MP, Pawlik JR (2017) Nutrient Fluxes and Ecological Functions of Coral Reef Sponges in a Changing Ocean. Climate Change, Ocean Acidification and Sponges. Springer International Publishing, pp 373–410

de Goeij JM, van Oevelen D, Vermeij MJA, Osinga R, Middelburg JJ, de Goeij AFPM, Admiraal W (2013) Surviving in a Marine Desert: The Sponge Loop Retains Resources Within Coral Reefs. Science 342:108–110

Eddy SR (2008) A Probabilistic Model of Local Sequence Alignment That Simplifies Statistical Significance Estimation. PLoS Comput Biol 4:e1000069

Engelberts JP, Robbins SJ, de Goeij JM, Webster NS, Aranda M, Bell SC, Webster NS (2020) Characterization of a sponge microbiome using an integrative genome-centric approach. ISME J 14:1100–1110

Fiore CL, Baker DM, Lesser MP (2013) Nitrogen Biogeochemistry in the Caribbean Sponge, Xestospongia muta: A Source or Sink of Dissolved Inorganic Nitrogen? PLoS ONE 8:e72961

Fiore CL, Jessica KJ, Steinert G, Lesser MP (2020) Trait-based comparison of coral and sponge microbiomes. Sci Rep 10:2340

Fiore CL, Labrie M, Jarett JK, Lesser MP (2015) Transcriptional activity of the giant barrel sponge, *Xestospongia muta* Holobiont: molecular evidence for metabolic interchange. Front Microbiol 6:364

Freeman CJ, Thacker RW (2011) Complex interactions between marine sponges and their symbiotic microbial communities. Limnol Oceanogr 56:1577–1586

Fry B (2006) Stable isotope ecology. Springer, New York

Garate L, Sureda J, Agell G, Uriz MJ (2017) Endosymbiotic calcifying bacteria across sponge species and oceans. Sci Rep 7:43674

Germer J, Cerveau N, Jackson DJ (2017) The holo-transcriptome of a calcified early branching metazoan. Front Mar Sci 4:81

Ginsburg RN (1983) Geological and biological roles of cavities in coral reefs. In: Barnes DJ (ed) Perspectives on Coral Reefs. Australian Institute of Marine Sciences, Townsville, Australia, pp 148–153

Gutleben J, Koehorst JJ, McPherson K, Pomponi S, Wijffels RH, Smidt H, Sipkema D (2019) Diversity of tryptophan halogenases in sponges of the genus *Aplysina*. FEMS Microbiol Ecol 95:fiz108

Haase-Schramm A, Böhm F, Eisenhauer A, Dullo W-C, Joachimski MM, Hansen B, Reitner J (2003) Sr/Ca ratios and oxygen isotopes from sclerosponges: temperature history of the Caribbean mixed layer and thermocline during the Little Ice Age. Paleoceanogr Paleoclimat 18:3

Hentschel U, Piel J, Degnan SM, Taylor MW (2012) Genomic insights into the marine sponge microbiome. Nat Rev Microbiol 10:641–654

Kolasinski J, Rogers K, Frouin P (2008) Effects of acidification on carbon and nitrogen stable isotopes of benthic macrofauna from a tropical coral reef. Rap Comm Mass Spec 22:2955–2960

Lang JC, Hartman WD (1975) Sclerosponges: primary framework constructors on the Jamaican deep fore-reef. J Mar Res 33:223–231

Langille MGI (2018) Exploring Linkages between taxonomic and functional profiles of the human microbiome. mSystems 3:e00163-17

Langille MGI, Zaneveld J, Caporaso JG, McDonald D, Knights D, Reyes JA, Clemente JC, Burkepile DE, Thurber RLV, Knight R, Beiko RG, Huttenhower C (2013) Predictive functional profiling of microbial communities using 16S rRNA marker gene sequences. Nat Biotechnol 31:814

Lesser MP (2006) Benthicpelagic coupling on coral reefs: Feeding and growth of Caribbean sponges. J Exp Mar Bio Ecol 328:277–288

Lesser MP, Slattery M (2018) Sponge density increases with depth throughout the Caribbean. Ecosphere 9:e02525

Lesser MP, Slattery M, Leichter JJ (2009) Ecology of mesophotic coral reefs. J Exp Mar Bio Ecol 375:1–8

Lesser MP, Slattery M, Stat M, Ojimi M, Gates RD, Grottoli A (2010) Photoacclimatization by the coral Montastraea cavernosa in the mesophotic zone: light, food, and genetics. Ecology, 91, 990–1003.Lesser MP, Slattery M, Mobley CD (2018) Biodiversity and functional ecology of mesophotic coral reefs. Ann Rev Ecol Evol Syst 49:49–71

Lesser MP, Slattery M, Laverick JH, Macartney KJ, Bridge TC (2019) Global community breaks at 60 m on mesophotic coral reefs. Glob Ecol Biogeogr 28:1403–1416

Lesser MP, Mueller B, Pankey MS, Macartney KJ, Slattery M, Goeij JM (2020) Depth-dependent detritus production in the sponge, *Halisarca caerulea*. Limnol Oceanogr 65:1200–1216

Loya Y, Eyal G, Treibitz T, Lesser MP, Appeldoorn R (2016) Theme section on mesophotic coral ecosystems: advances in knowledge and future perspectives. Coral Reefs 35:1–9

Mackenzie GJ, Schaffner FC, Swart PK (2015) The stable isotopic composition of carbonate (C and O) and the organic matrix (C and N) in waterbird eggshells from South Florida: insights into feeding ecology, timing of egg formation, and geographic range. Hydrobiologia 743:89–108

McMurdie PJ, Holmes S (2015) Shiny-phyloseq: web application for interactive microbiome analysis with provenance tracking. Bioinformatics 31:282–283

McMurray SE, Stubler AD, Erwin PM, Finelli CM, Pawlik JR (2018) A test of the sponge-loop hypothesis for emergent Caribbean reef sponges. Mar Ecol Prog Ser 588:1–14

Morrow KM, Fiore CL, Lesser MP (2016) Environmental drivers of microbial community shifts in the giant barrel sponge, *Xestospongia muta*, over a shallow to mesophotic depth gradient. Environ Microbiol 18:2025–2038

Mueller B, de Goeij JM, Vermeij MJA, Mulders Y, van der Ent E, Ribes M, van Duyl FC (2014) Natural diet of coral-excavating sponges consists mainly of dissolved organic carbon (DOC). PLoS ONE 9:e90152

Muscatine L, Porter JW, Kaplan IR (1989) Resource partitioning by reef corals as determined from stable isotope composition - I. $\delta^{13}C$ of zooxanthellae and animal tissue vs depth. Mar Biol 100:185–193

Muscatine L, Kaplan IR (1994) Resource partitioning by reef corals as determined from stable isotope composition II. $\delta^{15}N$ of zooxanthellae and animal tissue versus depth. Pac Sci 48:304–312

Parada AE, Needham DM, Fuhrman JA (2016) Every base matters: Assessing small subunit rRNA primers for marine microbiomes with mock communities, time series and global field samples. Environ Microbiol 18:1403–1414

Parnell AC, Inger R, Bearhop S, Jackson AL (2010) Source partitioning using stable isotopes: coping with too much variation. PLoS ONE 5(3):e9672

Pawlik JR (2011) The chemical ecology of sponges on caribbean reefs: natural products shape natural systems. Bioscience 61:888–898

Pita L, Rix L, Slaby BM, Franke A, Hentschel U (2018) The sponge holobiont in a changing ocean: from microbes to ecosystems. Microbiome 6:46

Ren H, Sigman DM, Thunell RC, Prokopenko MG (2012) Nitrogen isotopic composition of planktonic foraminifera from the modern ocean and recent sediments. Limnol Oceanogr 57:1011–1024

Rix L, de Goeij JM, Mueller CE, Struck U, Middelburg JJ, van Duyl FC, Al-Horani FA, Wild C, Naumann MS, van Oevelen D (2016) Coral mucus fuels the sponge loop in warm- and cold-water coral reef ecosystems. Sci Rep 6:18715

Santavy DL, Willenz P, Colwell RR (1990) Phenotypic study of bacteria associated with the Caribbean sclerosponge, *Ceratoporella nicholsoni*. Appl Environ Microbiol 56:1750–1762

Schubert CJ, Nielsen B (2000) Effects of decarbonation treatments on $\delta^{13}C$ values in marine sediments. Mar Chem 72:55–59

Shih JL, Selph KE, Wall CB, Wallsgrove NJ, Lesser MP, Popp BN (2020) Trophic ecology of the tropical Pacific sponge *Mycale grandis* inferred from amino acid compound-specific isotopic analyses. Microb Ecol 79:495–510

Slaby BM, Hackl T, Horn H, Bayer K, Hentschel U (2017) Metagenomic binning of a marine sponge microbiome reveals unity in defense but metabolic specialization. ISME J 11:2465–2478

Slattery M, Lesser MP (2014) Allelopathy in the tropical alga *Lobophora variegata* (P haeophyceae): mechanistic basis for a phase shift on mesophotic coral reefs? J Phycol 50:493–505

Slattery M, Lesser MP (2015) Trophic ecology of sponges from shallow to mesophotic depths (3 to 150 m): Comment on Pawlik et al. (2015) Mar Ecol Prog Ser 527:275–279

Slattery M, Gochfeld DJ, Easson CG, O'Donahue LRK (2013) Facilitation of coral reef biodiversity and health by cave sponge communities. Mar Ecol Prog Ser 476:71–86

Slattery M, Lesser MP, Brazeau D, Stokes MD, Leichter JJ (2011) Connectivity and stability of mesophotic coral reefs. J Exp Mar Bio Ecol 408:32–41

Slattery M, Gochfeld DJ, Diaz MC, Thacker RW, Lesser MP (2016) Variability in chemical defense across a shallow to mesophotic depth gradient in the Caribbean sponge *Plakortis angulospiculatus*. Coral Reefs 35:11–22

Swart PK, Greer L, Rosenheim BE, Moses CS, Waite AJ, Winter A, Dodge RE, Helmle K (2010) The ^{13}C Suess effect in scleractinian corals mirror changes in the anthropogenic CO_2 inventory of the surface oceans. Geophys Res Lett 37:5

Swart PK, Rubenstone JL, Charles C, Reitner J (1998) Sclerosponges : A new proxy indicator of climate. NOAA Climate and Global Change Program: Special Report 12:19

Swart PK, Thorrold S, Rosenheim B, Eisenhauer A, Harrison CGA, Grammer M, Latkoczy C (2002) Intra-annual variation in the stable oxygen and carbon and trace element composition of sclerosponges. Paleoceanogr Paleoclimat 17:1045

Taylor MW, Radax R, Steger D, Wagner M (2007) Sponge-associated microorganisms: evolution, ecology, and biotechnological potential. Microbiol Mol Biol Rev 71:295–347

Thomas T, Moitinho-Silva L, Lurgi M, Björk JR, Easson C, Astudillo-García C, Olson JB, Erwin PM, López-Legentil S, Luter H, Chaves-Fonnegra A, Costa R, Schupp PJ, Steindler L, Erpenbeck D, Gilbert J, Knight R, Ackermann G, Victor Lopez J, Taylor MW, Thacker RW, Montoya JM, Hentschel U, Webster NS (2016) Diversity, structure and convergent evolution of the global sponge microbiome. Nat Commun 7:1–12

Trindade-Silva AE, Rua CPJ, Andrade BGN, Vicente ACP, Silva GGZ, Berlinck RGS, Thompson FL (2013) Polyketide synthase gene diversity within the microbiome of the sponge Arenosclera brasiliensis, endemic to the southern Atlantic Ocean. Appl Environ Microbiol 79:1598–1605

Trussell GC, Lesser MP, Patterson MR, Genovese SJ (2006) Depth-specific differences in growth of the reef sponge *Callyspongia vaginalis*: role of bottom-up effects. Mar Ecol Prog Ser 323:149–158

van Duyl FC, Moodley L, Nieuwland G, van Ijzerloo L, van Soest RWM, Houtekamer M, Meesters EH, Middelburg JJ (2011) Coral cavity sponges depend on reef-derived food resources: stable isotope and fatty acid constraints. Mar Biol 158:1653–1666

van Duyl FC, Mueller B, Meesters EH (2018) Spatio-temporal variation in stable isotope signatures (δ13C and δ15N) of sponges on the Saba Bank. PeerJ 2018:1–25

Vacelet J, Willenz P, Hartman WD (2015) Living hypercalcified sponges: Treatise on invertebrate palaeontology, part E(revised), Porifera, vol. 4–5, pp. 1–14. Lawrence, KS: The University of Kansas Palaeontological Institute

Yahel G, Sharp JH, Marie D, Häse C, Genin A (2003) In situ feeding and element removal in the symbiont-bearing sponge *Theonella swinhoei*: Bulk DOC is the major source for carbon. Limnol Oceanogr 48:141–149

Ye Y, Doak TG (2009) A parsimony approach to biological pathway reconstruction/inference for genomes and metagenomes. PLoS Comput Biol 5:e1000465